LUND UNIVERSITY

Time-resolved x-ray scattering from laser-molten indium antimonide.

Nüske, Ralf; v Korff Schmising, C; Jurgilaitis, Andrius; Enquist, Henrik; Allaf Navirian, Hengameh; Sondhauss, Peter; Larsson, Jörgen

Published in:
Review of Scientific Instruments

DOI:
10.1063/1.3290418

2010

Link to publication

Citation for published version (APA):
Nüske, R., v Korff Schmising, C., Jurgilaitis, A., Enquist, H., Allaf Navirian, H., Sondhauss, P., & Larsson, J. (2010). Time-resolved x-ray scattering from laser-molten indium antimonide. *Review of Scientific Instruments*, *81*(1), Article 013106. https://doi.org/10.1063/1.3290418

Total number of authors:
7

General rights
Unless other specific re-use rights are stated the following general rights apply:
Copyright and moral rights for the publications made accessible in the public portal are retained by the authors and/or other copyright owners and it is a condition of accessing publications that users recognise and abide by the legal requirements associated with these rights.
• Users may download and print one copy of any publication from the public portal for the purpose of private study or research.
• You may not further distribute the material or use it for any profit-making activity or commercial gain
• You may freely distribute the URL identifying the publication in the public portal

Read more about Creative commons licenses: https://creativecommons.org/licenses/

Take down policy
If you believe that this document breaches copyright please contact us providing details, and we will remove access to the work immediately and investigate your claim.

LUND UNIVERSITY

PO Box 117
221 00 Lund
+46 46-222 00 00

AIP | Review of Scientific Instruments

Time-resolved x-ray scattering from laser-molten indium antimonide

R. Nüske, C. v. Korff Schmising, A. Jurgilaitis, H. Enquist, H. Navirian et al.

Citation: Rev. Sci. Instrum. **81**, 013106 (2010); doi: 10.1063/1.3290418
View online: http://dx.doi.org/10.1063/1.3290418
View Table of Contents: http://rsi.aip.org/resource/1/RSINAK/v81/i1
Published by the American Institute of Physics.

Additional information on Rev. Sci. Instrum.

Journal Homepage: http://rsi.aip.org
Journal Information: http://rsi.aip.org/about/about_the_journal
Top downloads: http://rsi.aip.org/features/most_downloaded
Information for Authors: http://rsi.aip.org/authors

ADVERTISEMENT

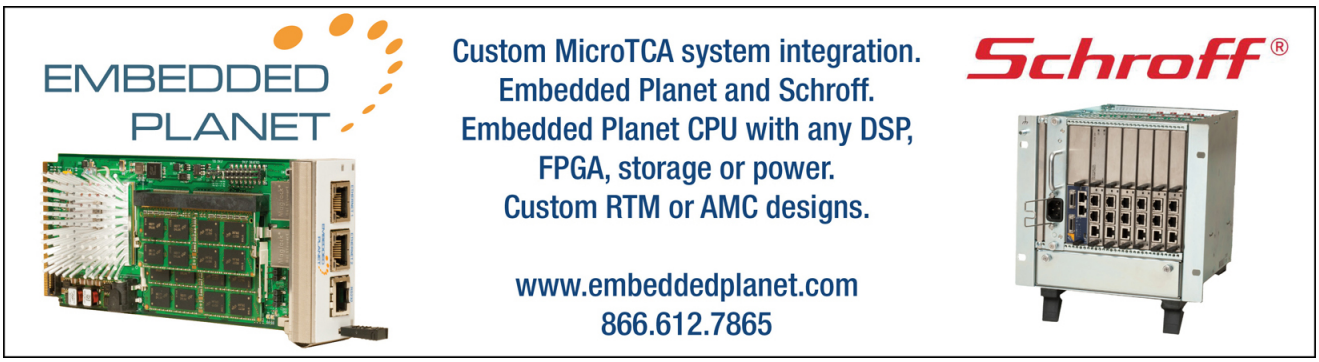

Downloaded 29 May 2012 to 130.235.184.47. Redistribution subject to AIP license or copyright; see http://rsi.aip.org/about/rights_and_permissions

Time-resolved x-ray scattering from laser-molten indium antimonide

R. Nüske, C. v. Korff Schmising, A. Jurgilaitis, H. Enquist, H. Navirian, P. Sondhauss, and J. Larsson
Department of Physics, Atomic Physics Division, Lund University, P.O. Box 118, Lund SE-221 00, Sweden

(Received 13 November 2009; accepted 16 December 2009; published online 22 January 2010)

We demonstrate a concept to study transient liquids with picosecond time-resolved x-ray scattering in a high-repetition-rate configuration. Femtosecond laser excitation of crystalline indium antimonide (InSb) induces ultrafast melting, which leads to a loss of the long-range order. The remaining local correlations of the liquid result in broad x-ray diffraction rings, which are measured as a function of delay time. After 2 ns the liquid structure factor shows close agreement with that of equilibrated liquid InSb. The measured decay of the liquid scattering intensity corresponds to the resolidification rate of 1 m/s in InSb. © *2010 American Institute of Physics.*
[doi:10.1063/1.3290418]

I. INTRODUCTION

Significant advances have been made in picosecond and subpicosecond time-resolved x-ray scattering techniques during the past decade. Experimental efforts have mainly been focused on the observation of nonthermal melting[1–3] and optical and acoustic phonon motion[4–8] in *crystalline* solids, while x-ray studies of transient states of *disordered* materials, e.g., liquids, have remained a greater experimental challenge. In contrast to strong Bragg reflections from crystalline material, the liquid state exhibits only weak x-ray scattering amplitudes due to the short correlation length of the disordered structure. The broad features of the liquid structure factor give insight into nearest-neighbor distances and occupation numbers, i.e., directly encode the local structure. Time-resolved liquid x-ray scattering experiments have allowed precise measurements of the reaction pathway of molecules in solution,[9–12] and have shed light on the dynamic structural changes of liquid water.[13] The emergence of the liquid phase of InSb after laser-driven nonthermal melting was recently captured directly with femtosecond resolution at the SPPS at the SLAC National Accelerator Laboratory.[14] This study focused on potential voids and ablated material which occur in the scattering pattern at low momentum transfer vectors. It was found that the liquid is formed within 1 ps. Simultaneously, Bragg peaks, indicative of an ordered lattice, disappeared.

In this letter we demonstrate the possibility of carrying out laser-pump/x-ray probe experiments using a two-dimensional (2D) detector at a synchrotron radiation facility with 10 ns bunch spacing and a uniform filling pattern, and report on laser-molten InSb and its subsequent regrowth with a temporal resolution of 400 ps.

II. SETUP FOR TIME-RESOLVED X-RAY SCATTERING

The time-resolved, liquid scattering experiment was carried out at beam line D611 at the MAX-laboratory synchrotron radiation facility in Lund, Sweden. X rays from a bending magnet of the 1.5 GeV MAX-II storage ring are focused by a toroidal gold-coated mirror and reduced in aperture by a set of slits. The small x-ray incident angle ($\theta_S = 0.9 \pm 0.05°$) leads to an elongated x-ray footprint of 0.1×3.0 mm^2. The x-ray divergence is 3×0.7 m rad^2 (horizontal·vertical), and a multilayer monochromator allows the energy to be set to $E_{\mathrm{x\ ray}} = 7.5$ keV with a bandwidth of $\Delta E_{\mathrm{x\ ray}}/E_{\mathrm{x\ ray}} = 10^{-2}$. A single x-ray probe pulse at the sample contains about 700 photons, and has a duration of approximately 300 ps.

A Ti:Al_2O_3-based femtosecond laser system, operating at a repetition rate of 4.25 kHz, with a 790 nm center wavelength, 4.5 W average power and 45 fs pulse duration, was used for excitation. The optical pump beam was focused by two cylindrical lenses to a spot size of 0.3×4.0 mm^2 [(full width at half maximum (FWHM)] which, assuming a Gaussian beam shape, yielded a fluence of 45 mJ/cm^2 incident on the sample. The laser pulses are synchronized to a particular electron bunch in the storage ring with a jitter below 10 ps.

A. Detection system

To study the diffuse scattering of the liquid phase of InSb a single-photon-counting detection system was designed and set up as shown in Fig. 1. The scattered x rays are converted into visible radiation (center wavelength $\lambda = 425$ nm) in a 2-mm-thick plastic scintillator (Saint Gobain, BC-408). The scintillator features a 2.1 ns decay time ($1/e$), and a 0.9 ns rise time (10%–90%), which corresponds to a total 2.5 ns pulse width (FWHM). The conversion efficiency was measured and found to be 60 photons per single 7.5 keV x-ray photon. The spatial resolution of the scintillator for x-ray detection is limited due to the deviations from normal incidence for x rays onto the scintillator and its thickness. This effect sets a lower limit for the Q resolution of the detector. In our case, the spatial resolution is 0.27 mm close to the beamstop, and 2.8 mm at the outer edge of the scintillator. This corresponds to 0.02–0.20 Å^{-1}. The Q resolution in our experiment is limited to 0.4 Å^{-1} at $Q = 3$ Å^{-1} due to the size of the x-ray spot. A thin aluminum coating (<500 nm) on the front of the scintillator blocks any stray light from the pump beam and reflects the generated visible

 © 2010 American Institute of Physics

Downloaded 29 May 2012 to 130.235.184.47. Redistribution subject to AIP license or copyright; see http://rsi.aip.org/about/rights_and_permissions

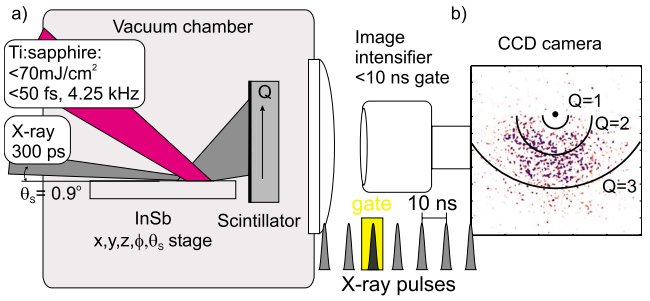

FIG. 1. (Color online) (a) Concept of the time-resolved liquid x-ray scattering setup. The broad scattering rings of liquid InSb are detected by a plastic scintillator. An image intensifier is used to electronically gate single x-ray bunches to achieve a time resolution of one x-ray bunch length plus the timing jitter between the x rays and laser radiation, i.e., approximately 350 ps. b) A typical 2D image of the liquid structure factor at $t=2$ ns; the lines indicate the equivalent scattering vectors, Q.

light toward the detection system. The generated photons from the scintillator are collected with a lens of 7.5 cm focal length and 15 cm diameter at 30 cm distance and imaged onto the photocathode of an image intensifier unit (Hamamatsu C9546). This results in a collection efficiency of 1.4%. The overall image magnification from the scintillator onto the charge-coupled device (CCD) is 1/9. The spatial resolution of the intensifier unit is 45 Lp/mm.

The image intensifier provides signal amplification and has a gating mode with gate times as short as 3 ns, i.e., it allows the selection of a single x-ray bunch synchronized to the laser repetition rate at 4.25 kHz. The minimum available gate time would be short enough to gate out single bunches at synchrotrons with rf frequencies up to 500 MHz, and 2 ns bunch spacing respectively. A scintillator with a sufficiently short pulse width, such as barium fluoride, would be required in this case.

To reach single x-ray photon sensitivity, a second (identical) image intensifier was connected in series, which allowed single, clearly distinguishable scattered x-ray photons to be counted. The maximum photon gain of the intensifier units at the emission wavelength of the scintillator (425 nm) is 3.8×10^3. The first intensifier was set to gating mode with high gain (900 V), and the second image intensifier was set to moderate gain (700 V) in continuous mode. The accessible voltage range is 600–1000 V.

The 2D scattered intensity is recorded using a thermoelectrically cooled Electron Multiplying CCD camera (Andor iXon). The sensor was cooled to −70 °C and the electron multiplying gain factor was set to 100. In conjunction with the gain from the image intensifiers, single x-ray photon sensitivity was reached. The CCD pixel size is 8 μm, the chip area is 8×8 mm^2.

The gain of the detector is sufficient to clearly detect single x-ray photon events. A single photon counting algorithm is used in the data analysis, which limits the signal-to-noise ratio to the shot noise level.

A realistic estimate for the quantum efficiencies of the components can be done as follows: The x-ray absorption at 7.5 keV in the scintillator is 64% and it converts on average into 60 photons, of which 1.4% is collected with the lens. The optical components used transmit in total 74% of the photons at the scintillators emission wavelength 425 nm. The image intensifier is specified with a quantum efficiency of 10% at the emission wavelength of the scintillator. All in all, it results in a total of 3.9%.

We determined the overall quantum efficiency of the detector using a strongly attenuated Bragg reflection of InSb. The x-ray flux before the scintillator is measured using a calibrated Si x-ray diode (AXUV100GX, International Radiation Detectors) and compared to the x-ray count rate on the 2D detector when the diode is removed. The overall detection efficiency (i.e., the ratio between scattered and detected photons) is measured to be 3.2%.

This detection technique eliminates the necessity for x-ray choppers to select a single x-ray pulse for time resolved x-ray scattering experiments.[15] A hybrid or single bunch filling pattern in the storage ring is not required. It offers a unique alternative to the gateable area pixel array detector PILATUS (gate time 150 ns), which was recently tested in time-resolved x-ray experiments.[16]

III. EXPERIMENTAL RESULTS

An InSb wafer [asymmetrically cut at −17° to the (1 1 1) planes] is mounted on a motorized xyz stage, which also allows θ_S and the azimuthal angle φ to be set remotely. The grazing incident geometry allows the x-ray penetration depth, $\xi_{\mathrm{x\ ray}}$ ($\approx$90 nm for $\theta_S=0.9°$ and $E_{\mathrm{x\ ray}}=7.5$ keV) and the melting depth ξ_{melt} to be matched.[14]

Over 100 short exposures with an acquisition times of 5 s alternating with "laser on" and "laser off" settings were measured. This means that the same surface area was molten more than 10^6 times. In order to investigate if this repetitive melting affects the data, we measured the total counts as a function of measuring time. We observed a moderate sublinear increase ($\propto t^{0.6}$) in the total counts as a function of measuring time. In high-repetition-rate melting experiments with moderate melting fluences (<45 mJ/cm^2) the only observed degeneration is the emergence of small ripple structures below 100 nm in height.[17] Such small surface structures do not adversely affect the scattering geometry, i.e., the matching of the x ray and laser penetration depth.

To control the spatial and temporal overlap of the x-ray probe and the optical pump, the decrease of the intensity of a strong Bragg reflection, e.g., (1 1 1) at $Q=1.68$ Å^{-1}, is monitored. The Bragg condition for different reflections is fulfilled by changing the azimuth angle φ and/or tuning the x-ray energy.[18] We tuned the x-ray energy to 5.4 keV on resonance with the (1 1 1) Bragg reflection from the asymmetrically cut InSb crystal. The gate of the image intensifier is set to include a single x-ray bunch shortly after excitation. If the overlap is good, a decrease in scattered intensity of about 40% is easily detected during an integration time of several seconds. This technique is also used to determine the time-delay zero. During the measurement of the scattering signal from liquid InSb, the Bragg reflection used for the overlap check was attenuated beyond the point where it could be detected, by tuning the x-ray energy off resonance to 7.5 keV. Figure 1(b) shows an example of an image of the difference signal of the integrated laser on and laser off mea-

Downloaded 29 May 2012 to 130.235.184.47. Redistribution subject to AIP license or copyright; see http://rsi.aip.org/about/rights_and_permissions

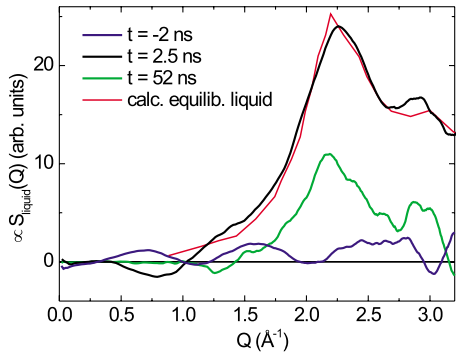

FIG. 2. (Color online) Liquid structure factor $S(Q)$ at various time delays: −2, +2.5, and 52 ns in respect to the laser pulse. Good agreement is seen with an *ab initio* calculation of equilibrated liquid InSb (solid line) (Ref. 19).

surements. The black lines indicate equivalent scattering vectors Q, where $Q=4\pi\cdot\sin(\theta)/\lambda$, with the scattering angle 2θ and the x-ray wavelength λ. Q space is calibrated by recording several low-indexed Bragg reflections of InSb. Integration yields the scattering intensity as a function of Q, which is shown in Fig. 2 for different time delays: 2 ns prior, 2.5 ns after, and 52 ns after the laser excitation. Here, the measured number of photons is corrected for the atomic form factor squared and, hence, yields a value directly proportional to the structure factor $S(Q)$. The first broad diffraction ring has its maximum at $Q=2.2$ Å^{-1}. This is in excellent agreement with an *ab initio* calculation for liquid InSb (red line) for $1<Q<3$ Å^{-1}.[19] However, the shoulder at approximately $Q=3$ Å^{-1} is more pronounced in the measurement.

Figure 3 shows the integrated scattering intensity for the main and the second peak at $Q=3$ Å^{-1} (inset) as a function of delay time. The intensity of the main peak increases more slowly than the temporal resolution of the experiment, and reaches a maximum after approximately 2 ns. It then falls to zero within 100 ns. The integrated scattering intensity of the second peak shows identical temporal behavior within the margin of uncertainty.

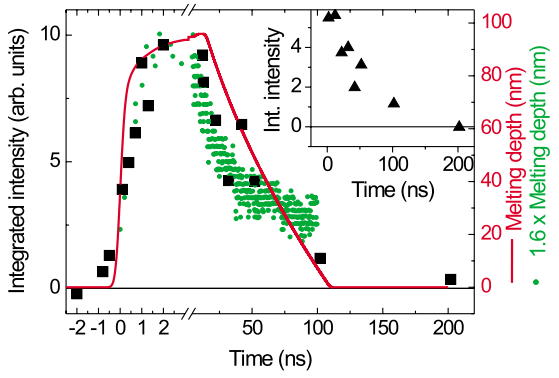

FIG. 3. (Color online) Integrated structure factor $S(Q)$ as a function of time delay. The squares and triangles (inset) correspond to the integrated structure factors of the peak at $Q=2.2$ Å^{-1} and $Q=3$ Å^{-1}, respectively. The melting depth as a function of time (solid line) was calculated using a 1D heat flow equation and reproduces the initial, noninstantaneous melting and the subsequent regrowth of InSb well. Experimental melting depths extracted from a nonthermal melting experiment conducted at a laser fluence of 36 mJ/cm^2 are also shown (dots) (Ref. 21).

IV. DISCUSSION

The good agreement between the integrated, scattered intensity and previously measured and calculated structure factors of equilibrated liquid InSb (Ref. 19) suggests that already after 2 ns the laser-formed liquid has a local structure similar to that of thermalized liquid InSb. Figure 2 shows background-corrected integrated, scattering intensities. The curve for a x-ray bunch 2 ns prior the laser excitation represents the overall noise level for this experiment, since the sample had sufficient time to resolidify and thermalize after the previous laser pulse. The curve for the delay of 2.5 ns shows the integrated scattering intensity from the liquid InSb when it is close to its maximum. After 52 ns the signal has dropped due to resolidification.

The shoulder of the structure factor at $Q=3$ Å^{-1} originates from the second nearest neighbor, at $r=4.3$ Å, of the crystalline zinc blende structure of InSb, and has been interpreted as a covalent Sb–Sb bond in liquid InSb.[19] This pronounced feature is well reproduced in our time-resolved measurements; its decay time unambiguously shows that it indeed arises from liquid InSb (cf. inset of Fig. 3). Because outer coordination shells generally disappear with increasing temperature,[20] this feature strongly corroborates the rapid thermalization of laser-molten InSb, i.e., within approximately 2 ns. More precisely, the temporal evolution of the scattering intensity is well explained by a simple one-dimensional (1D) heat flow model (red line in Fig. 3). Noting, that up to the probe depth, $\xi_{\mathrm{x\ ray}}\approx 90$ nm, the liquid scattering intensity is, to a first approximation, directly proportional to the melting depth, the model identifies the following four time regions of the transient liquid InSb. First, the energy deposited by the laser excitation leads to ultrafast, nonthermal melting of a surface layer with a thickness of $\xi_{\mathrm{melt}}\approx 50\pm 10$ nm.[1] In the second time region, the initial, high temperature gradient then results in rapid redistribution of energy and to subsequent thermal melting of deeper lying layers. This thermally molten volume contributes significantly to the measured scattered intensity, and leads to a noninstantaneous increase within approximately 2 ns. The high standard enthalpy of fusion of InSb initially causes an approximately 130-nm-thick layer at the constant melting temperature, $T_{\mathrm{melt}}=800$ K, directly below the molten surface layer, ξ_{melt}. This delays the conduction of heat and causes the plateau seen in the melting depth in the third time region between 3 and 15 ns. The decrease in the liquid scattering intensity during the subsequent fourth time region corresponds to the resolidification of InSb at a rate of approximately 1 m/s. The model shows best agreement with the measurements when a static sample temperature of 600 K is assumed.[21] In previous laser-induced melting experiments the formation of the liquid state was inferred by studying the ultrafast decrease of intensity in Bragg reflections,[1,21] providing complementary information about time-dependent melting depths. Data from Harbst *et al.*[21] are shown in Fig. 3 as green dots. We attribute the smaller melting depth reported by Harbst *et al.* compared to the simulation of the present experimental conditions to weaker laser excitation

Downloaded 29 May 2012 to 130.235.184.47. Redistribution subject to AIP license or copyright; see http://rsi.aip.org/about/rights_and_permissions

(36 mJ/cm^2 compared to 45 mJ/cm^2 in this study). The temporal characteristics reported by Harbst *et al.* are in excellent agreement with our data.

V. SUMMARY

In conclusion, we have demonstrated that time-resolved x-ray scattering experiments on laser-molten disordered InSb can be carried out at a synchrotron radiation facility with a uniform bunch fill pattern. Excellent agreement with previously determined liquid structure factors has been shown. The measured rise and decay times of the liquid scattering amplitude correspond to continued thermal melting and subsequent resolidification, respectively.

ACKNOWLEDGMENTS

The authors would like to thank the Swedish Research Council (VR), the Knut and Alice Wallenberg Foundation, the Crafoord Foundation, the Carl Trygger Foundation, and the European Commission via the Marie Curie Programme for their financial support.

[1] A. Rousse, C. Rischel, S. Fourmaux, I. Uschmann, S. Sebban, G. Grillon, P. Balcou, E. Foster, J. P. Geindre, P. Audebert, J. C. Gauthier, and D. Hulin, Nature (London) **410**, 65 (2001).
[2] K. Sokolowski-Tinten, C. Blome, C. Dietrich, A. Tarasevitch, M. H. von Hoegen, D. von der Linde, A. Cavalleri, J. Squier, and M. Kammler, Phys. Rev. Lett. **87**, 225701 (2001).
[3] A. M. Lindenberg, J. Larsson, K. Sokolowski-Tinten, K. J. Gaffney, C. Blome, O. Synnergren, J. Sheppard, C. Caleman, A. G. MacPhee, D. Weinstein, D. P. Lowney, T. K. Allison, T. Matthews, R. W. Falcone, A. L. Cavalieri, D. M. Fritz, S. H. Lee, P. H. Bucksbaum, D. A. Reis, J. Rudati, P. H. Fuoss, C. C. Kao, D. P. Siddons, R. Pahl, J. Als-Nielsen, S. Duesterer, R. Ischebeck, H. Schlarb, H. Schulte-Schrepping, T. Tschentscher, J. Schneider, D. von der Linde, O. Hignette, F. Sette, H. N. Chapman, R. W. Lee, T. N. Hansen, S. Techert, J. S. Wark, M. Bergh, G. Huldt, D. van der Spoel, N. Timneanu, J. Hajdu, R. A. Akre, E. Bong, P. Krejcik, J. Arthur, S. Brennan, K. Luening, and J. B. Hastings, Science **308**, 392 (2005).
[4] A. M. Lindenberg, I. Kang, S. L. Johnson, T. Missalla, P. A. Heimann, Z. Chang, J. Larsson, P. H. Bucksbaum, H. C. Kapteyn, H. A. Padmore, R. W. Lee, J. S. Wark, and R. W. Falcone, Phys. Rev. Lett. **84**, 111 (2000).
[5] K. Sokolowski-Tinten, C. Blome, J. Blums, A. Cavalleri, C. Dietrich, A. Tarasevitch, I. Uschmann, E. Forster, M. Kammler, M. Horn-von Hoegen, and D. von der Linde, Nature (London) **422**, 287 (2003).
[6] M. Bargheer, N. Zhavoronkov, Y. Gritsai, J. C. Woo, D. S. Kim, M. Woerner, and T. Elsaesser, Science **306**, 1771 (2004).
[7] P. Beaud, S. L. Johnson, A. Streun, R. Abela, D. Abramsohn, D. Grolimund, F. Krasniqi, T. Schmidt, V. Schlott, and G. Ingold, Phys. Rev. Lett. **99**, 174801 (2007).
[8] C. von Korff Schmising, M. Bargheer, M. Kiel, N. Zhavoronkov, M. Woerner, T. Elsaesser, I. Vrejoiu, D. Hesse, and M. Alexe, Phys. Rev. Lett. **98**, 257601 (2007).
[9] A. Plech, M. Wulff, S. Bratos, F. Mirloup, R. Vuilleumier, F. Schotte, and P. A. Anfinrud, Phys. Rev. Lett. **92**, 125505 (2004).
[10] H. Ihee, M. Lorenc, T. K. Kim, Q. Y. Kong, M. Cammarata, J. H. Lee, S. Bratos, and M. Wulff, Science **309**, 1223 (2005).
[11] J. Vincent, M. Andersson, M. Eklund, A. B. Wohri, M. Odelius, E. Malmerberg, Q. Kong, M. Wulff, R. Neutze, and J. Davidsson, J. Chem. Phys. **130**, 154502 (2009).
[12] M. Christensen, K. Haldrup, K. Bechgaard, R. Feidenhans'l, Q. Kong, M. Cammarata, M. L. Russo, M. Wulff, N. Harrit, and M. M. Nielsen, J. Am. Chem. Soc. **131**, 502 (2009).
[13] A. M. Lindenberg, Y. Acremann, D. P. Lowney, P. A. Heimann, T. K. Allison, T. Matthews, and R. W. Falcone, J. Chem. Phys. **122**, 204507 (2005).
[14] A. M. Lindenberg, S. Engemann, K. J. Gaffney, K. Sokolowski-Tinten, J. Larsson, P. B. Hillyard, D. A. Reis, D. M. Fritz, J. Arthur, R. A. Akre, M. J. George, A. Deb, P. H. Bucksbaum, J. Hajdu, D. A. Meyer, M. Nicoul, C. Blome, Th. Tschentscher, A. L. Cavalieri, R. W. Falcone, S. H. Lee, R. Pahl, J. Rudati, P. H. Fuoss, A. J. Nelson, P. Krejcik, D. P. Siddons, P. Lorazo, and J. B. Hastings, Phys. Rev. Lett. **100**, 135502 (2008).
[15] M. Cammarata, L. Eybert, F. Ewald, W. Reichenbach, M. Wulff, P. Anin-rud, F. Schlotte, A. Plech, Q. Kong, M. Lorenc, B. Lindenau, J. Räbiger, and S. Polachowski, Rev. Sci. Instrum. **80**, 015101 (2009).
[16] T. Ejdrup, H. T. Lemke, K. Haldrup, T. N. Nielsen, D. A. Arms, D. A. Walko, A. Miceli, E. C. Landahl, E. M. Dufresne, and M. M. Nielsen, J. Synchrotron Radiat. **16**, 387 (2009).
[17] H. Navirian, H. Enquist, T. N. Hansen, A. Mikkelsen, P. Sondhauss, A. Srivastava, A. A. Zakharov, and J. Larsson, J. Appl. Phys. **103**, 103510 (2008).
[18] J. Larsson, O. Synnergren, T. N. Hansen, K. Sokolowski-Tinten, S. Werin, C. Caleman, J. Hajdu, J. Sheppard, J. S. Wark, A. M. Lindenberg, K. J. Gaffney, and J. B. Hastings, *Second International Conference on Photo-Induced Phase Transitions: Cooperative, Nonlinear and Functional Properties, Journal of Physics Conference Series*, Opportunities and Challenges Using Short-Pulse X-Ray Sources Vol. 21, edited by M. Buron and E. Collet (Institute of Physics, Bristol, 2005).
[19] C. Q. Zhang, Y. H. Wei, and C. F. Zhu, Chem. Phys. Lett. **408**, 348 (2005).
[20] Q. Wang, C. X. Li, Z. H. Wu, L. W. Wang, X. J. Niu, W. S. Yan, Y. N. Xie, S. Q. Wei, and K. Q. Lu, J. Chem. Phys. **128**, 224501 (2008).
[21] M. Harbst, T. N. Hansen, C. Caleman, W. K. Fullagar, P. Jonsson, P. Sondhauss, O. Synnergren, and J. Larsson, Appl. Phys. A: Mater. Sci. Process. **81**, 893 (2005).

Downloaded 29 May 2012 to 130.235.184.47. Redistribution subject to AIP license or copyright; see http://rsi.aip.org/about/rights_and_permissions